S-Transform–Based Time–Frequency Analysis of Backscattered Acoustic Signals

Youssef Nahraoui [1*], *Samir* Elouaham[2], and *Aassif* Elhoucein[1]
[1]LMTI, Faculty of Sciences of Agadir, Ibn Zohr University, Agadir, P.O. Box 8106, Morocco
[2]LISTI, National School of Applied Sciences, Ibn Zohr University, Agadir, Morocco

Abstract. Acoustic scattering offers a reliable non-destructive route for investigating submerged monolayer cylindrical shells, enabling wall thickness, material properties, and degradation effects to be inferred without compromising structural integrity. Among the most informative descriptors, the reduced cut-off frequency of the antisymmetric circumferential guided mode A_1 is particularly attractive because it is highly sensitive to geometric variations and material contrast, providing a compact indicator for condition monitoring. Here, we employ a time–frequency analysis based on the S-transform to enhance modal energy localization in the backscattered response and to extract the A_1 reduced cut-off frequency under noisy conditions. The cut-off is identified by detecting the first statistically significant energy ridge after band selection and robust normalization. The extracted values show close agreement with resonance eigenmode theory over a broad range of configurations described by the radius ratio b/a, where a and b denote the outer and inner radii, respectively. Overall, these results demonstrate that S-transform-based cut-off tracking provides an efficient framework for reduced-frequency characterization of submerged cylindrical shells.

1 Introduction

Metallic tubes (e.g., copper and steel) are ubiquitous in heat exchangers and fluid-transport networks. In submerged service, corrosion/erosion and fluid loading modify their vibro-acoustic response, making in-situ non-destructive ultrasonic assessment essential. Under plane-wave incidence, an air-filled tube in water excites circumferential guided modes that satisfy resonance conditions at discrete frequencies, producing sharp peaks in the backscattered spectrum. These resonances, indexed by the circumferential order n, form symmetric S_i and antisymmetric A_i families analogous to Lamb waves in plates [1]. Because the dimensionless (reduced) resonance features depend strongly on geometry—particularly the radius ratio b/a (with a and b the outer and inner radii)—they provide an acoustic fingerprint for characterizing submerged shells.

Prior work has advanced analytical and numerical descriptions of submerged shells and scattering, including models for double-walled shells [2], data-driven predictors of circumferential-wave behaviour [3,4]. Maze et al. [1,5] also introduced MIIR and formalized the shell–plate analogy that supports the interpretation of S_i and A_i families. Nevertheless, practical identification remains challenging because classical frequency-domain processing largely relies on isolating resonance peaks from the form function, which offers limited direct access to the emergence of modes and can become ambiguous when peaks overlap, broaden under damping, or are contaminated by noise. Time–frequency representations such as the Wigner–Ville distribution can reveal dispersive content more clearly [6], but cross-terms and sensitivity to noise may hinder reliable extraction of physically meaningful parameters [7].

To address these limitations, we employ time–frequency analysis based on the S-Transform to estimate the reduced cutoff frequency of the antisymmetric A_1mode, a key parameter for cylindrical-shell characterization. Compared with Wigner–Ville–type approaches, the S-Transform provides a localized, multiresolution mapping with reduced interference artefacts, while preserving interpretable time–frequency localization. This enables robust identification of the A_1 modal onset (cutoff) from the backscattered response, even in the presence of noise and closely spaced resonances, thereby providing a compact and geometry-sensitive descriptor for submerged cylindrical shells.

2 Physical and Mathematical Formulation of Acoustic Scattering

Scattering by an air-filled cylindrical shell submerged in water (sound speed C_1) and parameterized by the radius ratio $b/a$is described by the wave equation subject to the corresponding boundary conditions [1,8]. For normal plane-wave incidence, an acoustic field of angular frequency $\omega$and wavenumber $k_1 = \omega/C_1$impinges on an infinitely long shell whose axis coincides with the z-axis of the cylindrical coordinate system (r, Θ, z), as illustrated in Fig. 1. In the far field, the complex backscattered pressure can be expressed through a normal-mode expansion that separates the main echo components—namely the

* Corresponding author: nahraouissef@gmail.com

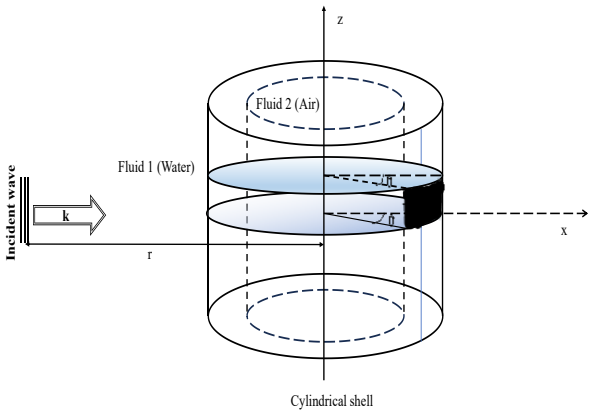

Fig. 1. Configuration of an air-filled tube immersed in water under normal plane-wave incidence.

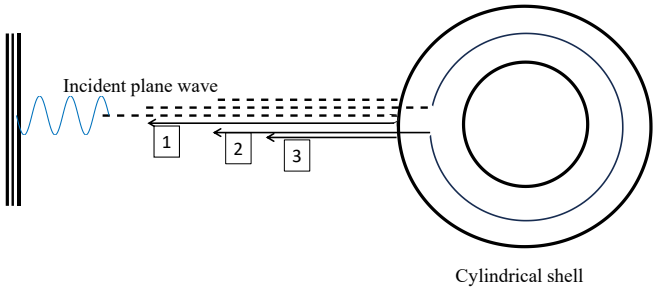

Fig. 2. Main contributions to the backscattered signal: (1) specular reflection, (2) circumferential guided-wave component, and (3) interfacial Scholte wave (A mode).

Table 1. Physical and material parameters considered in this study.

	Copper	Water (Fluid 1)	Air (Fluid 2
Density ρ (kg/m^3)	8930	1000	1.29
C_L: Longitudinal velocity (m/s)	4760	1470	334
C_T: Transverse Velocity (m/s)	2325	----------	---------- --

specular contribution (1), the shell-guided circumferential waves of whispering-gallery/Rayleigh type (2), and the interfacial Scholte wave (3)—as illustrated in **Fig. 2**. A Sommerfeld–Watson transform further classifies the circumferential guided waves into symmetric $S_0, S_1, \ldots$and antisymmetric branches (Scholte A, $A_0, A_1, \ldots$) [8, 9]. The scattered pressure in a plane normal to $z$is written as [5,10]:

$$P_{scat}(\omega) = P_0 \frac{1-i}{\sqrt{\pi k_1 r}} expi(k_1 - \omega t) \times \sum_{n=0}^{n} \varepsilon_n \frac{D_n^1(\omega)}{D_n(\omega)} \cos(n\theta) \quad (1)$$

where P_0 denotes the incident-wave amplitude, $\omega$is the angular frequency, and $k_1 = \omega/C_1$is the acoustic wavenumber in the external fluid with sound speed C_1. The parameter $r$is the emitter–receiver distance measured from the tube axis, $\varepsilon_n = 1$ for $n = 0$ and $\varepsilon_n = 2$ for $n \neq 0$, and $D_n(\omega)$ and $D_n^1(\omega)$ are frequency-dependent determinants resulting from enforcing the boundary conditions at the two interfaces. In accordance with the experimental time-gating procedure, a shifted time origin is introduced as:

$$t' = t + t_1, \quad (2)$$

with the water time-of-flight

$$t_1 = \frac{r}{C_1} = \frac{u+a}{C_1}, \quad (3)$$

where u is the stand-off distance and a is the outer radius. With this substitution, the far-field pressure at the transducer location becomes:

$$P_{scat}(\omega) = P_0 \frac{1-i}{\sqrt{\pi k_1 r}} expi(2k_1 a) \times expi(2k_1 u - \omega t') \sum_{n=0}^{n} \varepsilon_n \frac{D_n^1(\omega)}{D_n(\omega)} \cos(n\theta) \quad (4)$$

In practice, the oscilloscope time axis is shifted so that the scattered contribution starts at the acquisition window, yielding:

$$2k_1 u - \omega t' = 0, \quad (5)$$

and therefore:

$$P_{scat}(\omega) = P_0 \frac{1-i}{\sqrt{\pi k_1 r}} expi(2k_1 a) \times \sum_{n=0}^{n} \varepsilon_n \frac{D_n^1(\omega)}{D_n(\omega)} \cos(n\theta) \quad (6)$$

Results are commonly reported versus the reduced (dimensionless) frequency:

$$x_1 = k_1 a = \frac{2\pi \nu a}{C_1}, \quad (7)$$

where ν denotes the acoustic frequency in hertz. The associated time-domain signal is subsequently reconstructed by taking the inverse Fourier transform:

$$P_{\text{scat}} = \int_{-\infty}^{+\infty} h(\omega)\ P_{\text{scat}}(\omega) \exp(-i\omega t)\, d\omega, \quad (8)$$

where $h(\omega)$ is the transducer band-pass. Experimentally, the specular echo is removed by time-windowing (replaced by zeros), and the resonance spectrum is obtained by Fourier transforming the specular-suppressed signal [1,5]. For example, a submerged copper tube $(b/a = 0.90)$ exhibits resonance peaks associated with circumferential modes of order n; plotting the trajectories $n(x_1)$ organizes them into the Scholte branch A, the symmetric S_0 family, and the antisymmetric A_1 family, with A_1 showing a low-order cutoff (Figs. 3–4) [1,8–9].

3 S-Transform Formulation

The S-transform can be introduced in several ways. Here, it is convenient to view it as a continuous wavelet transform (CWT) augmented by a frequency-dependent phase factor, i.e., a "phase-corrected" CWT. The continuous wavelet transforms (CWT) of a signal $h(t)$, denoted $W(\tau, d)$, is defined as:

$$W(\tau, d) = \int_{-\infty}^{+\infty} h(t)\, \omega(t - \tau, d)\, dt, \quad (9)$$

where $\omega(t, d)$ is a scaled version of the mother wavelet. The dilation parameter $d$controls the effective width of $\omega(t, d)$ and thus determines the time–

frequency resolution. In the CWT framework, the mother wavelet is required to satisfy an admissibility condition. [11], in particular the zero-mean constraint. Comprehensive reviews can be found in Rioul and Vetterli [12] and Young [13]. Accordingly, the S-transform of $h(t)$is obtained from a CWT using a specific wavelet and an additional phase factor:

$$S(\tau, f) = e^{i2\pi f\tau}\, W(\tau, d), \tag{10}$$

where the wavelet is defined as

$$\omega(t, f) = \frac{|f|}{\sqrt{2\Pi}} e^{\frac{-t^2 f^2}{2}} e^{-2\Pi f t} \tag{11}$$

In this formulation, the dilation is set to $d = 1/|\, f\, |$. However, the wavelet given in (11) does not strictly fulfill the zero-mean condition; consequently, expression (10) departs from the standard CWT definition when admissibility is enforced.

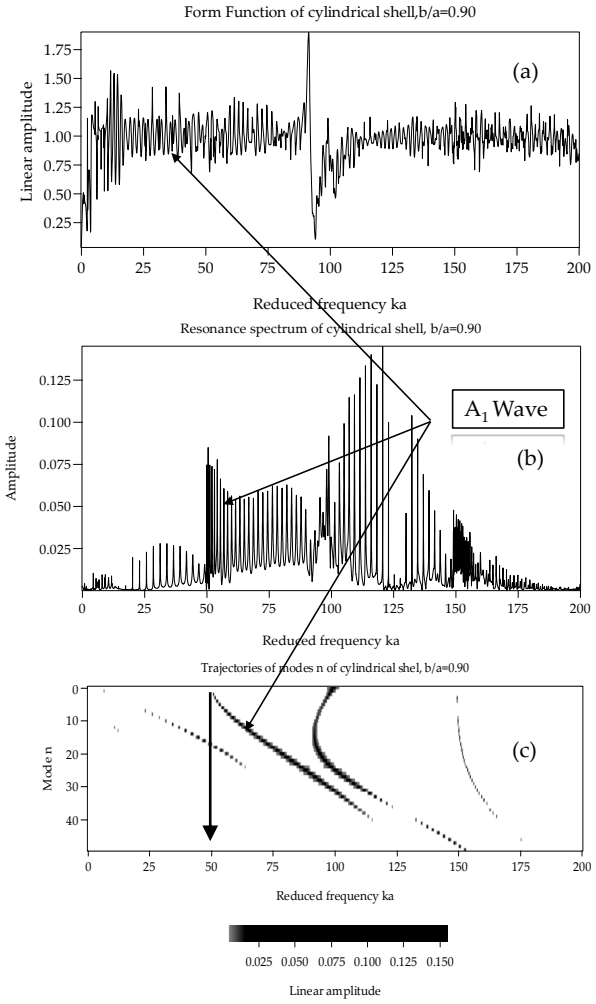

Fig.3. Frequency-dependent localization of circumferential waves in a submerged copper cylindrical shell ($b/a = 0.90$): (a) time-domain backscattered pressure signal, (b) corresponding resonance spectrum, and (c) evolution of the circumferential modal order $n$as a function of the reduced frequency. Vertical arrows indicate the correspondence between the step-like transitions observed in (a) and the resonance peaks identified in (b). The vertical line denotes the dimensionless cut-off frequency of the antisymmetric A_1mode.

not strictly a CWT. Written explicitly, the S transform is:

$$S(\tau, f) = \int_{-}^{+} h(t) \frac{|f|}{\sqrt{2\Pi}} e^{\frac{-(\tau - t)^2 f^2}{2}} e^{-2\Pi f t} dt \tag{12}$$

Viewing the S-transform as a local spectral representation implies that time-averaging should reproduce the Fourier spectrum; accordingly, one can show that

$$\int_{-\infty}^{+\infty} S(\tau, f)\, d\tau = H(f), \tag{13}$$

where $H(f)$ denotes the Fourier transform of $h(t)$. It follows that $h(t)$ is exactly recoverable from $S(\tau, f)$, i.e.,

$$h(t) = \int_{-\infty}^{+\infty} \left(\int_{-\infty}^{+\infty} S\,(\tau, f)\, d\tau \right) e^{i2\pi f t}\, df \tag{14}$$

This property distinguishes the S transform from standard CWT representations.

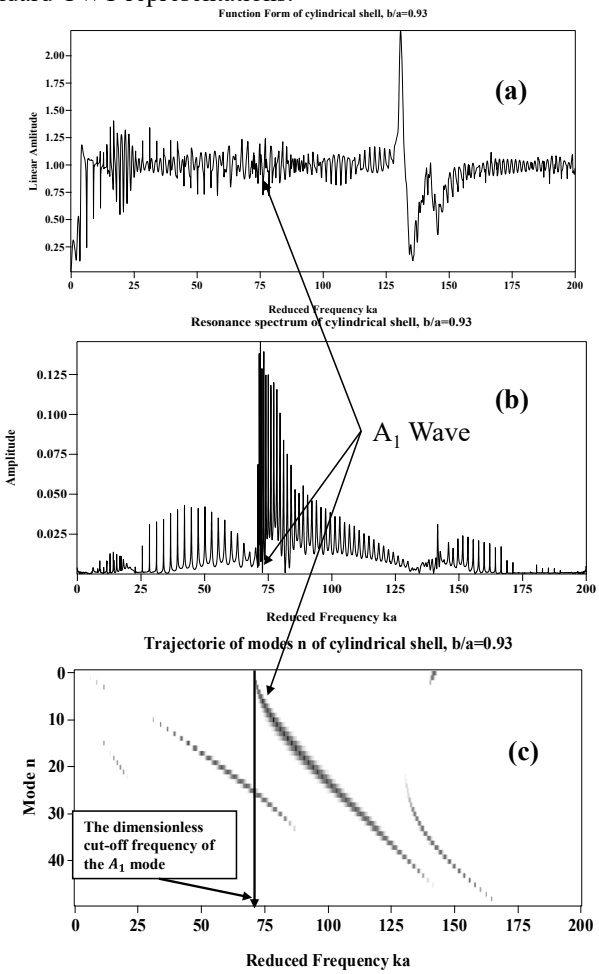

Fig.4. Frequency-dependent localization of circumferential waves in a submerged copper cylindrical shell ($b/a = 0.93$): (a) time-domain backscattered pressure signal, (b) corresponding resonance spectrum, and (c) evolution of the circumferential modal order $n$as a function of the reduced frequency. Vertical arrows indicate the correspondence between the step-like transitions observed in (a) and the resonance peaks identified in (b). The vertical line denotes the dimensionless cut-off frequency of the antisymmetric A_1mode.

In addition, the S-transform offers a broadband generalization of instantaneous frequency (IF) [14]. When $f = f_1$is held constant, $S(\tau, f_1)$defines a *voice*, in the CWT sense, and takes the form:

$$S(\tau, f_1) = A(\tau, f_1)\, e^{i\phi(\tau, f_1)} \tag{15}$$

By virtue of its component-selective nature, a voice allows the instantaneous frequency to be inferred from

the phase term $\phi(\tau, f_1)$, consistent with Bracewell's formulation [24]:

$$\mathrm{IF}(\tau, f_1) = \frac{1}{2\pi}\frac{d}{d\tau}(2\pi f_1 \tau + \phi(\tau, f_1)) \quad (16)$$

Therefore, the availability of an absolutely referenced phase provides a broadband extension of Bracewell's instantaneous frequency. The validity of (16) can be readily checked for the elementary case $h(t) = \cos(2\pi w t)$, which yields $\Phi(\tau, f) = 2\pi(w - f)\tau$. In addition, because the S-transform is linear, an additive-noise model of the form $\mathrm{data}(t) = \mathrm{signal}(t) + \mathrm{noise}(t)$ implies that

$$S\{\mathrm{data}\} = S\{\mathrm{signal}\} + S\{\mathrm{noise}\}.$$

Practical implementation. For a discrete-time signal $h[n]$ sampled at frequency f_s, the S transform is evaluated on a discrete frequency grid $f_k = kf_s/N$ to obtain a time–frequency representation $S[n, k]$. Owing to the frequency-dependent Gaussian window ($d = \frac{1}{|f|}$), the S transform provides a multi-resolution analysis with enhanced frequency localization at low frequencies and improved time localization at high frequencies.

4 Results and Discussion

Earlier studies employed time–frequency analysis based on Wigner–Ville representations (and smoothed variants) to estimate reduced cut-off frequencies from the backscattered acoustic response, and these cut-off estimates were subsequently integrated into data-driven frameworks (e.g., fuzzy-logic systems) to support identification under varying thickness conditions. Related work further showed that, once reliable time–frequency features are available, learning-based schemes (e.g., neural networks) can be trained to predict dispersive quantities of circumferential waves over a range of b/avalues [15].

In the present results, Figs. 5–6 indicate that the S-Transform provides a cleaner and more interpretable localization of modal energy after specular-echo suppression, band limiting, and robust normalization. In particular, the antisymmetric A_1contribution—often weak in the raw time trace—emerges as a coherent energy ridge in the time–frequency plane. From the time–frequency images obtained by applying the S-Transform, the reduced cut-off frequency can be estimated as the intersection between the A_1asymptotic trend and the frequency axis, expressed in reduced-frequency form X; for instance, $X = 49.16$ corresponds to the A_1reduced cut-off for a tube with radius ratio $b/a = 0.93$ See Fig. 5. The extracted reduced cut-off values agree closely with resonance eigenmode theory across the investigated b/a range, while larger deviations occur mainly when the A_1 energy is low, modal crowding increases, or damping broadens and partially overlaps nearby spectral features. Overall, these findings show that S-Transform-based ridge tracking yields a robust, physically interpretable estimate of the A_1reduced cut-off frequency, providing an efficient reduced-frequency descriptor for submerged cylindrical shells and improved tolerance to noise and experimental variability compared with peak-based spectral inspection.

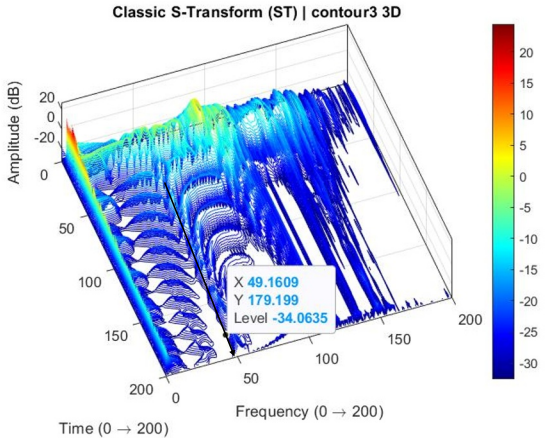

Fig.5 S-Transform time–frequency representation of the backscattered signal for a cylindrical shell with $b/a = 0.90$.

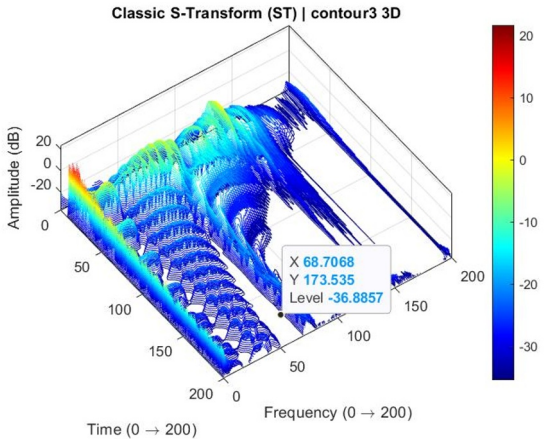

Fig.6 S-Transform time–frequency representation of the backscattered signal for a cylindrical shell with $b/a = 0.93$.

5 references

[1] G. Maze, J. L. Izbicki, and J. Ripoche, "Resonances of plates and cylinders: Guided waves," J. Acoust. Soc. Amer., vol. 77, pp. 1352–1357, 1985.

[2] Xiangwen Luo, Haibo Zhou, Lin Li, Hengxu Liu, Yeqing Jin, Jeom Kee Paik, 'Acoustic vibrations of underwater double-walled cylindrical shells with elastically restrained boundaries' Applied Ocean Research 154 (2025) 104426.

[3] Nahraoui, Y.; Aassif, E.H.; Elouaham, S.; Nassiri, B. A Fuzzy Model for Predicting the Group and Phase Velocities of Circumferential Waves Based on Subtractive Clustering. Signals 2025, 6, 56. https://doi.org/10.3390/signals6040056.

[4] Y. Nahraoui, E. H. Aassif, S. Elouaham and H. Banouni, "Prediction of the Phase Velocity of a Cylindrical Shell Immersed in Water by the Subtractive Clustering Approach Based on Sugeno Fuzzy Inference System," 2025 International Conference on Circuit, Systems and Communication (ICCSC), Fez, Morocco, 2025, pp. 1-5, doi: 10.1109/ICCSC66714.2025.11135441.

[5] Maze, G. Acoustic scattering from submerged cylinders. MIIR Im/Re: Experimental and

theoretical study. J. Acoust. Soc. Amer. 1991, 89, 2559–2566.

[6] Latif, R.; Aassif, E.; Maze, G.; Moudden, A.; Faiz, B. Determination of the group and phase velocities from time-frequency representation of Wigner-Ville. J. Non-Destr. Test. Eval. Int. 1999, 32, 415–422.

[7] Flax, L.; Dragonette, L.; Uberall, H. Theory of elastic resonance excitation by sound scattering. J. Acoust. Soc. Amer. 1978, 63, 723–731.

[8] G. V. Frisk, J. W. Dickey, and H. ¨ Uberall, "Surface wave modes on elastic cylinders," J. Acoust. Soc. Amer., vol. 58, pp. 996 1008, 1975.

[9] P. L. Marston and N. H. Sun, "Backscattering near the coincidence frequency of a thin cylindrical shell: Surface wave prop erties from elastic theory and an approximate ray synthesis," J. Acoust. Soc. Amer., vol. 97, pp. 777–783, 1995.

[10] Abdelilah Dariouchy, El Houcein Aassif, Dominique Décultot, and Gérard Maze ''Acoustic Characterization and Prediction of the Cut-Off Dimensionless Frequency of an Elastic Tube by Neural Networks'', IEEE transactions on ultrasonics, ferroelectrics, and frequency control, vol. 54, no. 5, may 2007.

[11] I. Daubechies, "The wavelet transform, time-frequency localization and signal analysis," IEEE Trans. Inform. Theory, vol. 36, no. 5, Sept. 1990.

[12] O. Rioul and M. Vetterli, "Wavelets and signal processing," IEEE Signal Processing Mag., vol. 8, pp. 14-38, 1991.

[13] R. K. Young, Wavelet Theory and Its Applications. Dordrecht: Kluwer, 1993.

[14] R. N. Bracewell, The Fourier Transform and Its Applications. New York McGraw-Hill, 1978.

[15] Y. NAHRAOUI, EL. AASSIF, G. MAZE, ''Prediction of the group velocity of acoustic circumferential waves by artificial neural network'' Journal of Theoretical and Applied Information Technology (JATIT) Vol.88. No.3 30th June 2016.